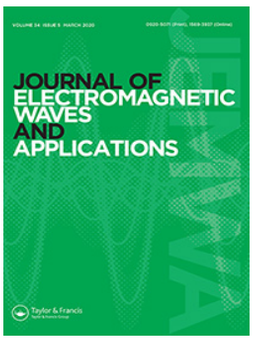

Taylor & Francis
Taylor & Francis Group

Journal of Electromagnetic Waves and Applications

ISSN: 0920-5071 (Print) 1569-3937 (Online) Journal homepage: https://www.tandfonline.com/loi/tewa20

Proof of the density tapering concept of an unequally spaced array by electric field distributions of electromagnetic simulations

Nguyen Quoc Dinh, Nguyen Thanh Binh, Yoshihide Yamada & Naobumi Michishita

To cite this article: Nguyen Quoc Dinh, Nguyen Thanh Binh, Yoshihide Yamada & Naobumi Michishita (2020) Proof of the density tapering concept of an unequally spaced array by electric field distributions of electromagnetic simulations, Journal of Electromagnetic Waves and Applications, 34:5, 668-681, DOI: 10.1080/09205071.2020.1736185

To link to this article: https://doi.org/10.1080/09205071.2020.1736185

JOURNAL OF ELECTROMAGNETIC WAVES AND APPLICATIONS
2020, VOL. 34, NO. 5, 668–681
https://doi.org/10.1080/09205071.2020.1736185

Proof of the density tapering concept of an unequally spaced array by electric field distributions of electromagnetic simulations

Nguyen Quoc Dinh[a], Nguyen Thanh Binh[a], Yoshihide Yamada[b] and Naobumi Michishita[c]

[a]Department of Radio-Electronics Engineering, Le Quy Don Technical University, Hanoi, Vietnam; [b]Malaysia-Japan International Institute of Technology UTM, Kuala Lumpur, Malaysia; [c]National Defense Academy, Yokosuka, Japan

ABSTRACT

The design method of an unequally spaced array was based on the density tapering in the textbook "Antenna theory" in 1969. The effects on grating lobe reductions were shown by radiation pattern calculations. However, no proof for the achievement of density tapering was shown. In this paper, through direct comparisons of the objective amplitude distribution with electric field distributions by electromagnetic simulation, density tapering is examined. A log-periodic dipole antenna operating from 900MHz to 2500MHz is designed for the array element. The unequally spaced 31-element array antenna is used for calculation. At many kinds of density tapering and many frequencies, calculated electric field distributions in a near-field region of the array antenna agree with the given density tapering distributions. The paper results show that the density tapering is achieved from 900MHz to 2000MHz and the effects of grating lobe reductions are ensured from 900MHz to 2500MHz.

ARTICLE HISTORY
Received 25 September 2019
Accepted 18 February 2020

KEYWORDS
Antenna gain; broadband antenna; density tapered array; grating lobe; log-periodic dipole antenna; multi-frequency; side lobe level; unequally spaced array

1. Introduction

Currently, next-generation mobile communication system (5G) is developing [1,2]. The requirements of antenna equipped at the base station are operational at millimetre wave band, multiple radiation beams and multi-frequency band. At 3G and 4G systems, multi-frequency band array antennas with equally element spacing are employed [3,4]. For multi-beam operation, special multi-beam feed circuits, such as Butler matrix [5] or Rotman lens [6] circuits, are used for elements feed. The problem of multi-beam operation of the equally spaced array is the appearance of grating lobe in the off-axis beams in the case of the element spacing more than 0.7 wavelengths, which is suppressed by the unequally spaced array [7]. The grating lobes produce interferences to other multi-beams. In previous research, to reduce grating lobe levels, unequally spaced array antenna was proposed by King et al. [8], Unz [9–11]. In addition, the low sidelobe characteristics of the unequally

CONTACT Nguyen Quoc Dinh dinhnq@mta.edu.vn

spaced array with uniform excitation to all array elements are also indicated by Harrington in [12] and others [13–17]. The systematic design method of the unequal array was shown in the textbook of "Antenna theory" [18]. Here, element spacing is called "density" and density taper design method to achieve the excitation amplitude taper is established. Justification for the similarity of element spacing taper to excitation amplitude taper was shown in the textbook by comparing two radiation patterns of density and amplitude methods. Now, electromagnetic simulations are used for the analysis of antenna performances. So, by direct comparisons of the electric field distribution of a density tapered array antenna with amplitude taper, justification of the density tapered array concept may be possible.

In this paper, through direct comparisons of the objective amplitude distribution with electric field distributions by electromagnetic simulation, density tapering concept is examined. In Section 2, the design method of density tapered spacing for an unequally spaced array antenna is explained. Herein, the cosine amplitude distribution function is taken as an example for determining the locations of array elements. In Section 3, designing of the log-periodic dipole antenna for array element use is explained. In Section 4, electromagnetic simulation results of electric field distributions of designed unequally spaced array antenna are shown. Comparisons of the given cosine amplitude distributions with calculated electric field distributions are made. Moreover, as for important features of the unequally spaced array antenna, grating lobe reduction effects in radiation patterns are shown.

2. Density tapered array

An unequal spaced elements synthesis method is introduced in [18]. The purpose is to achieve the given continuous amplitude taper distribution by the density tapered spacing of equal amplitude elements. The element location in the array is determined by the following process:

2.1. Equal-area approximation

The concept of the equal area approximation is shown in Figure 1. The function $f(x)$ is the given amplitude (current) distribution of an array antenna. The objective is to achieve $f(x)$ by unequal arrangement of element spacing. Here, excitation amplitudes of all the elements are equal. In order to achieve $f(x)$ by spacing, the assumption that multiply of Δx_i (spacing) and $f(x_i)$ at x_i point should be equal (equal-area, S) will be adequate.

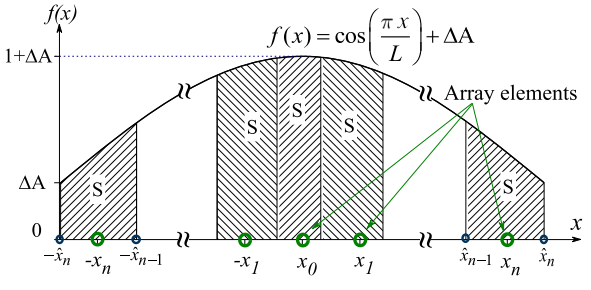

Figure 1. Concept of the equal-area approximation.

In order to determine the area S, the total area S_{all} can be calculated from the next equation.

$$S_{all} = \int_{-L/2}^{L/2} f(x)dx \tag{1}$$

where L is the continuous source dimension normalized to the wavelength.

The position of the array elements will be determined by dividing the S_{all} into N sub-areas, where N is the number of elements in an array. The relation between S_{all}, S, and N can be written as

$$S = \frac{S_{all}}{N} \tag{2}$$

In order to determine array element positions (x_i), boundary points $\{\pm\hat{x}_n, \ldots, \pm\hat{x}_0\}$, shown in Figure 1 are introduced. The boundary point $\hat{x}_i$ can be calculated by the next expression

$$\int_{-L/2}^{\hat{x}_i} f(x)dx = (n-i)S,$$
$$\text{where } \begin{cases} i = n, n-1, \ldots, 0, & N = 2n+1. \\ i = n, n-1, \ldots, 1, & N = 2n. \end{cases} \tag{3}$$

The element positions x_i are given by the next expression.

$$x_i = \frac{\hat{x}_i + \hat{x}_{i-1}}{2} \tag{4}$$

2.2. Design of density tapered spacing

In this paper, the cosine on pedestal current distribution given by the next expression will be considered.

$$f(x) = \cos\left(\frac{\pi x}{L}\right) + \Delta\mathrm{A}, \quad |x| \le \frac{L}{2} \tag{5}$$

Here, ΔA represents the value of the pedestal.

The $f(x)$ distributions of $\Delta\mathrm{A} = 0.5$ (DTA1), $\Delta\mathrm{A} = 0.3$ (DTA3) and $\Delta\mathrm{A} = 0.1$ (DTA5) are shown in Figure 2.

The total area is calculated as follows.

$$\begin{aligned} S_{all} &= \int_{-L/2}^{L/2} \left\{\cos\left(\frac{\pi x}{L}\right) + \Delta\mathrm{A}\right\} dx \\ &= 2L\left(\frac{1}{\pi} + \frac{\Delta\mathrm{A}}{2}\right). \end{aligned} \tag{6}$$

Then, the equal-area (S) becomes the next value.

$$S = \frac{2L}{N}\left(\frac{1}{\pi} + \frac{\Delta\mathrm{A}}{2}\right) \tag{7}$$

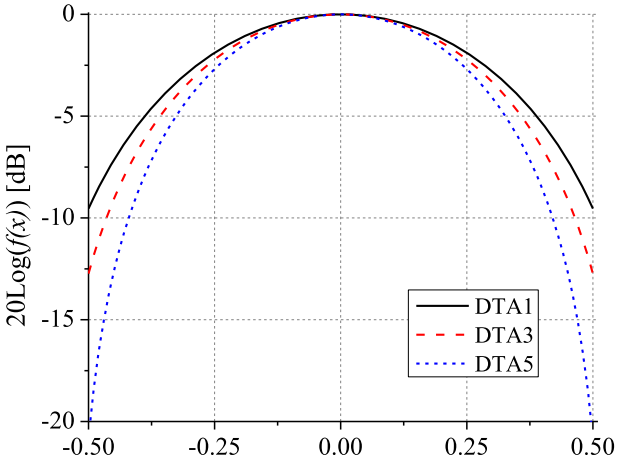

Figure 2. *f(x)* distribution for different ΔA values.

Next, by applying Equations (5) and (7) into Equation (3), the next expression that determines $\hat{x}_i$ is obtained.

$$\frac{L}{\pi}\left(1-\sin\left(\frac{\pi\hat{x}_i}{L}\right)\right)+\Delta A\left(\frac{L}{2}-\hat{x}_i\right) = (n-i)\left(\frac{1}{\pi}+\frac{\Delta A}{2}\right)\frac{2L}{N} \tag{8}$$

From Equations (8) and (4), it is easy to determine the boundary points $\hat{x}_i$ and elements position x_i.

2.3. Designed element position

To get the practical data for antenna array design, a frequency range from 900 to 2500 MHz is selected. When the number of elements in an array is set to $N = 31$ and the total length is fixed to $30 \times 0.7\lambda_{max}$, with λ_{max} is the wavelength at the lowest frequency ($f_{min} = 900$ MHz). The values of x_i in the case of the equally spaced array (ESA) and density tapered arrays (DTAs) with different values of ΔA are summarized in Table 1. The investigation frequencies and their wavelengths are shown in Table 2.

From the data of Table 1, the minimum and maximum spacing between two consecutive elements are given by the following equation:

$$\Delta x_i = (x_{i+1} - x_i)\left(\frac{\lambda_1}{\lambda}\right), \quad i = 0, 1, \ldots, 14. \quad \text{[wavelength]} \tag{9}$$

The minimum and maximum valued are inversely proportional to the wavelength shown by Equation (9). From the above equation, the minimum and maximum spacing at $\Delta A = 0.1$ (DTA5) in the frequency f_1 are 0.499 wavelengths at $i = 0$, and the maximum one is 1.695 wavelength at $i = 14$.

Table 1. Array elements location [normalized by λ_1].

Label	ESA	DTA1	DTA2	DTA3	DTA4	DTA5
$x[\lambda]$ / ΔA		0.5	0.4	0.3	0.2	0.1
x_0	0	0	0	0	0	0
x_1	0.700	0.547	0.538	0.527	0.515	0.499
x_2	1.400	1.097	1.078	1.056	1.033	1.006
x_3	2.100	1.651	1.622	1.590	1.554	1.515
x_4	2.800	2.212	2.174	2.131	2.083	2.030
x_5	3.500	2.783	2.735	2.681	2.621	2.555
x_6	4.200	3.366	3.309	3.244	3.172	3.092
x_7	4.900	3.965	3.899	3.824	3.739	3.646
x_8	5.600	4.585	4.510	4.424	4.328	4.220
x_9	6.300	5.231	5.147	5.052	4.944	4.822
x_{10}	7.000	5.911	5.820	5.715	5.596	5.459
x_{11}	7.700	6.634	6.538	6.426	6.295	6.144
x_{12}	8.400	7.416	7.318	7.201	7.063	6.898
x_{13}	9.100	8.282	8.188	8.073	7.932	7.756
x_{14}	9.800	9.276	9.202	9.106	8.979	8.805
x_{15}	10.500	10.500	10.500	10.500	10.500	10.500

Table 2. Calculation frequencies.

Frequency	f_1	f_2	f_3	f_4
[MHz]	900	1500	2000	2500
Wave Length	λ_1	λ_2	λ_3	λ_4
[mm]	333	200	150	120

Table 3. Description of a log-periodic dipole antenna.

Geometric ratio (τ)	0.77
Apex angles (2α)	50 (deg.)
Number of dipoles (N)	6
Diameter of dipoles (2a)	5 (mm)
Spacing of the feeder conductors (S)	6 (mm)
External transmission line impedance	50 (ohms)
Design frequency	900–2500 (MHz)

3. Array element design

3.1. Configuration of LPDA

In order to obtain broadband antenna, the log-periodic dipole antenna (LPDA) covers the wide frequency range from 900 to 2500 MHz employed as array elements. The design parameters of an LPDA are described in Table 3.

The relation between the dipole lengths (l_n) of the original log-periodic array is defined by the inverse of the geometric ratio τ as

$$\frac{1}{\tau} = \frac{l_{n+1}}{l_n}, \quad n = 1, 2, \ldots 5. \tag{10}$$

The structure of the LPDA is shown in Figure 3. From the element spacing data of Table 1, the spacing x_1 at the central element is smaller than the size of the original LPDA ($d_1 < l_6 = \lambda/2$). Hence, we cannot place correctly this antenna in the array. Therefore, the longest dipole (l_6) in the original LPDA is reduced by using a wire bow-ties

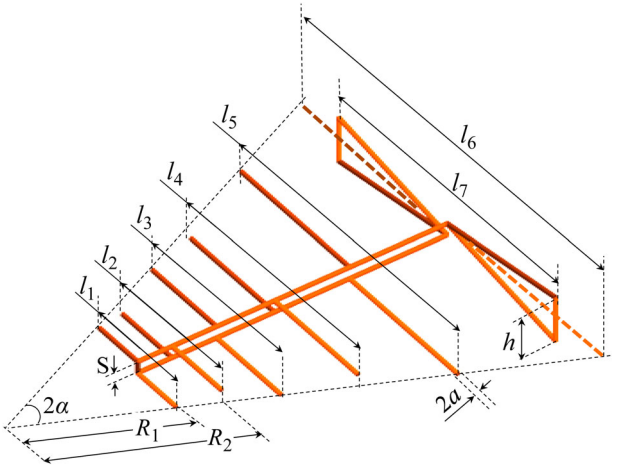

Figure 3. Geometry of a modified Log-periodic dipole antenna.

Table 4. Length and spacing of dipole elements.

Label	l_1	l_2	l_3	l_4	l_5	l_6	l_7	h
Length [mm]	45	59	76	99	128	166	128	19
Label	R_1	R_2	R_3	R_4	R_5	R_6		
Spacing [mm]	48	63	81	106	137	178		

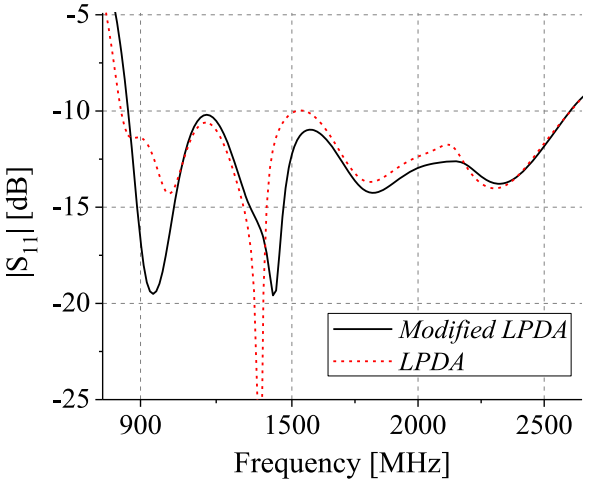

Figure 4. The return loss of LPDA and modified LPDA.

antenna, as shown in Figure 3. This antenna is called by name-modified LPDA. The particular dimensions of LPDA and modified LPDA are summarized in Table 4.

3.2. LPDA performances

Electric characteristics such as bandwidth, electric field distributions and radiation patterns are obtained. First, as for the bandwidth characteristics, the return loss ($|S_{11}|$) is calculated

(based on a 50-ohm line impedance) for an original LPDA and modified LPDA. The frequency characteristics of from 900 to 2500 MHz are shown in Figure 4. It becomes clear that the reflection coefficient is below −10 dB in the frequency range from 900 to 2500 MHz.

Next, electric field distributions in the near-field region are shown in Figure 5. The interesting tendency is observed that the strong field area exists near the antenna at 900 MHz.

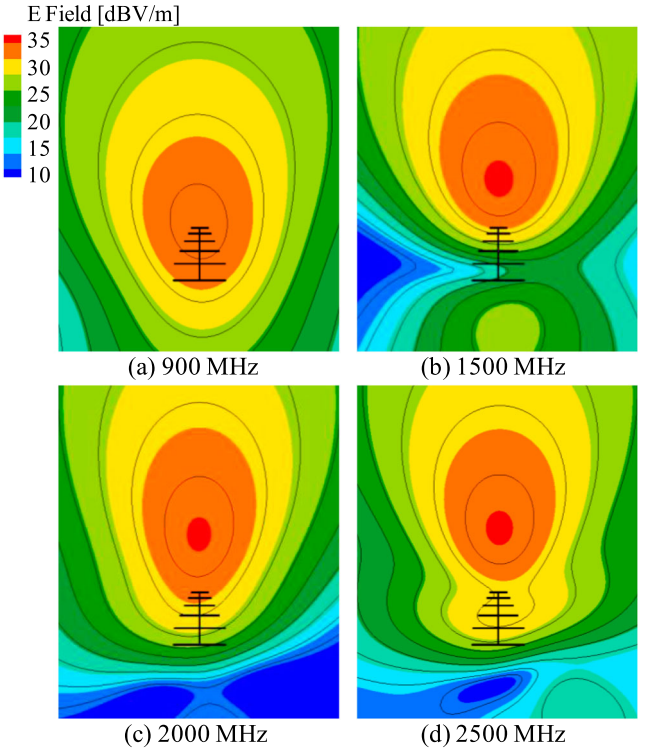

Figure 5. Electric field distributions in the near field.

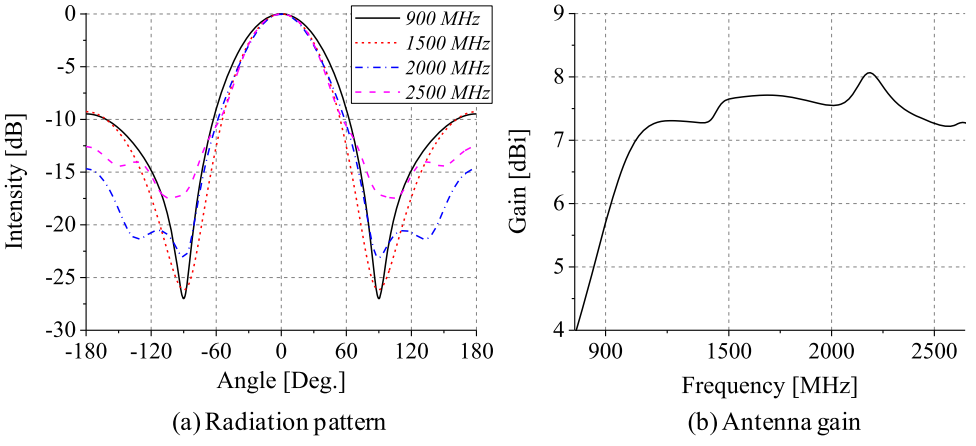

Figure 6. Radiation pattern and gain of a modified LPDA.

However, the strong field areas move toward the front side of the antenna in accordance with the frequency increases.

Radiation patterns of a modified LPDA in E-plane are shown in Figure 6(a). The beam widths become almost the same in the frequency range from 900 to 2500 MHz. Antenna gains are shown in Figure 6(b). At 900 MHz, antenna gain becomes 5.5 dBi. At 1500, 2000 and 2500 MHz, antenna gain becomes around 7.5 dBi.

4. Simulation results of the unequally spaced array

4.1. Configuration of the unequally spaced array antenna

The 31 elements array antenna structure is shown in Figure 7. Modified LPDA elements are arranged on the z-axis. Element spacing is settled based on the data of Table 1. Excitation

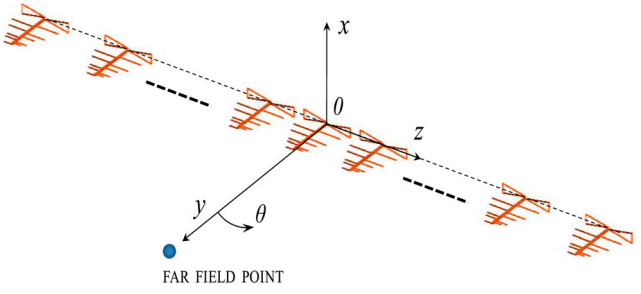

Figure 7. Configuration of density tapered array.

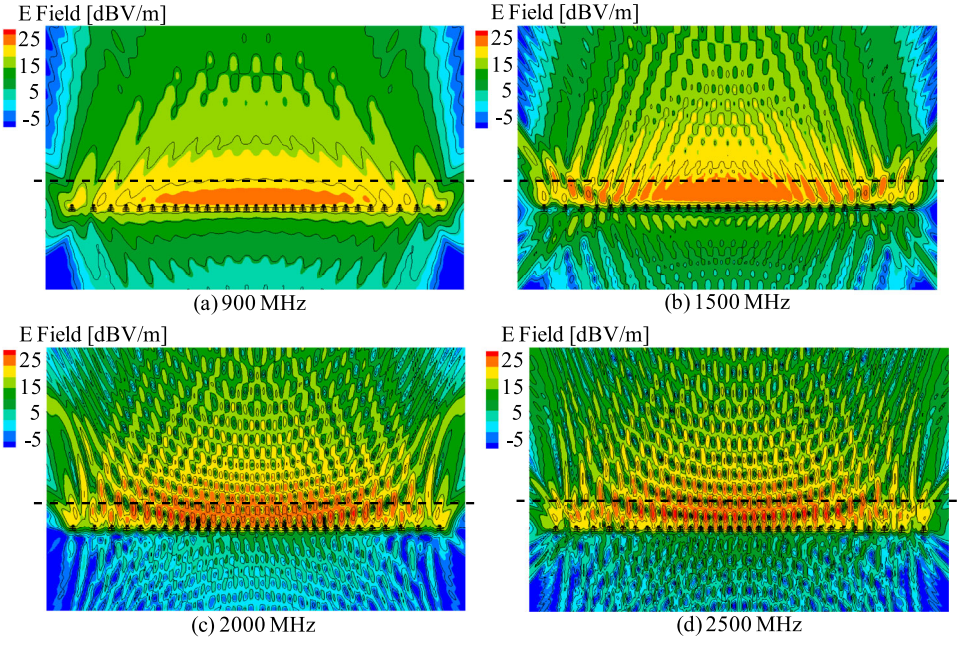

Figure 8. Electric field distributions of DTA1.

amplitude and phase for all elements are set constant. Excitation condition is set 1 watt for all elements.

4.2. Electric field distributions in the near field

Calculated electric field distributions at 900, 1500, 2000 and 2500 MHz are shown in Figure 8(a–d), respectively. Here, element spacing of DTA1 (small tapering) is employed in Table 1.

At 900 MHz data of Figure 8(a), it is observed that electric fields are tapering continuously in the element positions between $-x_{14}$ and x_{14}. Achievement of *f(x)* distribution of Figure 2 may be expected. At 1500 MHz of Figure 8(b), it is observed that electric fields are tapering continuously in the element positions between $-x_7$ and x_7. At the element positions outside $-x_8$ and x_8, electric field distributions become rippled. It is clear from the region of outside data in Tables 1 and 2, it is $-x_8$ and x_8, element spacing becomes larger than one wavelength at 1500 MHz. At 2000 and 2500 MHz data in Figure 8(c,d), all element spacing exceeds one wavelength. So, electric field distributions become rippled. However, the achievement of *f(x)* distribution of Figure 2 may be expected.

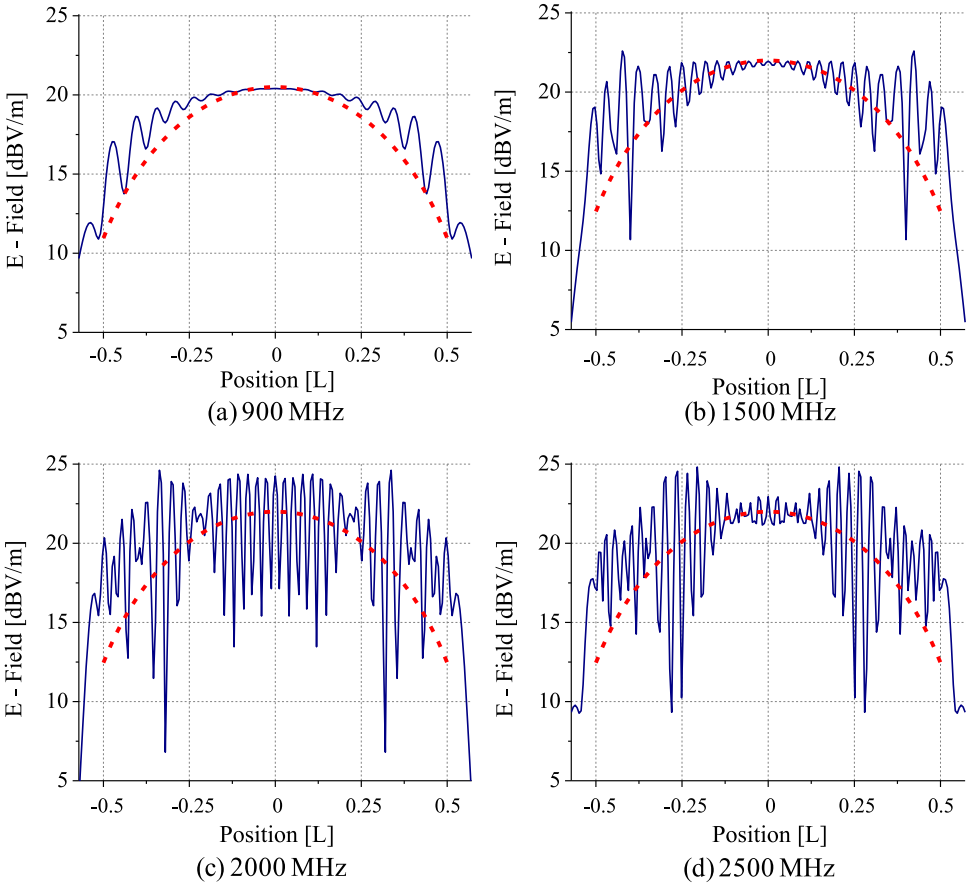

Figure 9. Comparisons of electric field distributions of DTA1 (solid line) versus density taper function (dashed line).

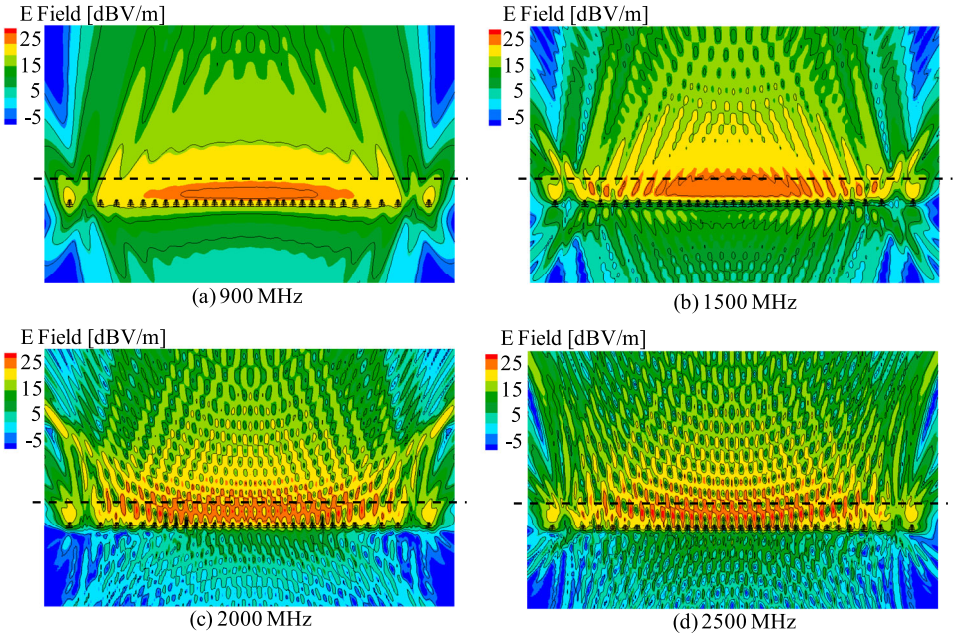

Figure 10. Electric field distributions of DTA5.

In order to examine the achievement of *f(x)* distribution of Figure 2, electric field tapering distributions are obtained from the data of Figure 8(a–d) at the place indicated by dashed lines. Comparisons of *f(x)* distributions and electric field tapering distributions are shown in Figure 9(a–d).

In the data of 900 MHz shown in Figure 9(a), deviations of electric field distribution are very small and agreement with the *f(x)* distribution (red colour dashes line) is rather well. The overall taper of the electric field distribution becomes small due to the mutual coupling between array elements. As a judgement, the achievement of the *f(x)* distribution by the density tapered spacing is confirmed. At the frequency 1500 MHz shown in Figure 9(b), deviations of electric field distribution become large at the array edge. However, averaged vales of electric fields agree well with the *f(x)* distribution. Here, the effect of mutual coupling that reduced taper of the electric field distribution. At the frequency 2000 MHz shown in Figure 9(c), deviations of electric field distribution become large. However, averaged vales of electric fields are comparable with the *f(x)* distribution. At the frequency 2500 MHz shown in Figure 9(d), deviations of electric field distribution become very large.

Another calculated results of DTA5 (large tapering) in Table 1 are shown in Figure 10(a–d). Electric field distributions are similar to the results of Figure 8. The difference is that the taper distributions of electric fields become stronger.

Comparisons of *f(x)* distributions and electric field tapering distributions of DTA5 (large tapering) are shown in Figure 11(a–d). The red dashed line shows the *f(x)* distribution. Deviations of the electric field distribution become large in accordance with the increase of frequency. The average value of the deviation can be comparable with the *f(x)* distribution. The taper of electric field distribution becomes smaller than *f(x)* because of mutual coupling between array elements.

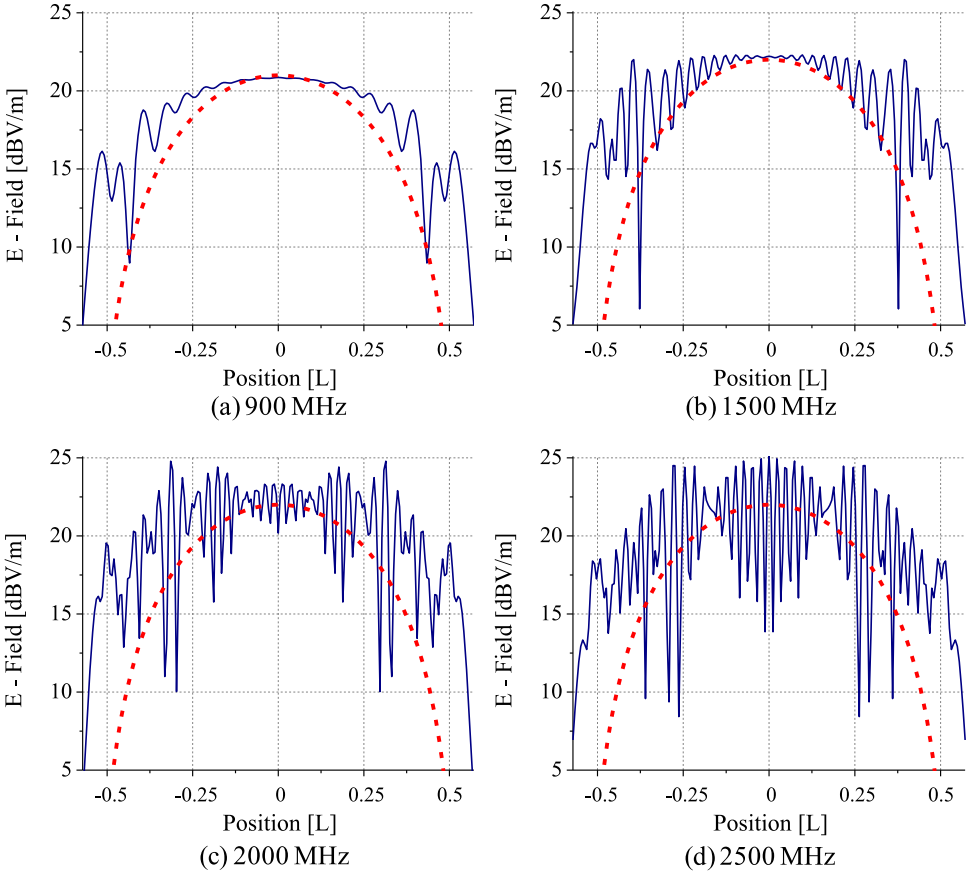

Figure 11. Comparisons of electric field distributions of DTA5 (solid line) versus density taper function (dash line).

From Figures 9 and 11, by taking into account the mutual coupling effect electric field distribution, the *f(x)* distribution is ensured by electric field distribution.

4.3. Radiation pattern

Here, the grating lobe suppression effect by the unequally spaced array antenna is examined. First, radiation patterns of equally spaced array antenna, whose element spacing is given by ESA of Table 1, are shown in Figure 12(a–d). At 900 MHz of Figure 12(a), because the element spacing is $0.7\lambda_{900}$, no grating lobe appears in the radiation pattern. At 1500 MHz of Figure 12(b), grating lobes appear at the angle $\theta_G = 59$ degree. At this frequency, element spacing (d) becomes $1.17\lambda_{1500}$. The relation of element spacing and grating lobe direction (θ_G) is given by the next equation.

$$d \times \sin(\theta_G) = \lambda_f$$

By putting $d = 1.17\lambda_{1500}$ in Equation (11), $\theta_G = 59$ degree is obtained. At frequencies 2000 and 2500 MHz that are shown in Figure 12(c,d), grating lobes appear at $\theta_G = 40$ and $\theta_G = 31$ degrees, respectively.

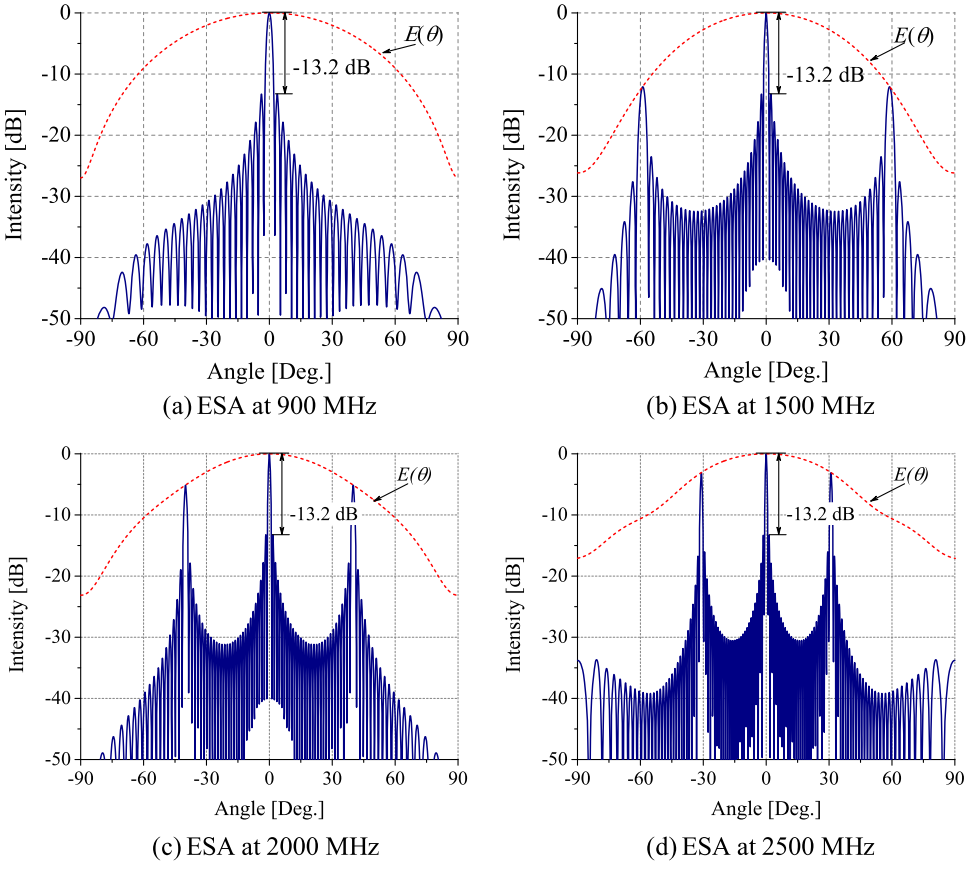

Figure 12. Radiation pattern of the equally spaced array.

Radiation patterns of unequally spaced array antenna, whose element spacing is given by DTA5 of Table 1, are shown in Figure 13(a,d). By comparing Figure 12(b,c,d) with Figure 13(b,c,d), it is clearly understood that grating lobes are sufficiently suppressed at 1500, 2000 and 2500 MHz, respectively. In Figure 13(a) 900 MHz, the far sidelobe levels are increased than those in Figure 12(a). However, the maximum level is below −22 dB. So, no serious problem may happen.

Antenna gain changes depending on frequencies are shown in Figure 14. It is interesting that no change of antenna gains happens between equally spaced and unequally spaced arrays. As for frequency dependences, gain increase from 900 to 1500 MHz seems natural. However, at 2000 and 2500 MHz, antenna gains are saturated. The reason for this saturation will be that grating lobes appear near the central beam.

5. Conclusion

In this paper, we propose a technique that is used a proof for the achievement of the density tapering concept is made by comparing the objective distribution function with the achieved electric field distributions. In calculation, a log-periodic dipole antenna operating at 900 to 2500 MHz is designed for the array element. The 31 elements unequally spaced

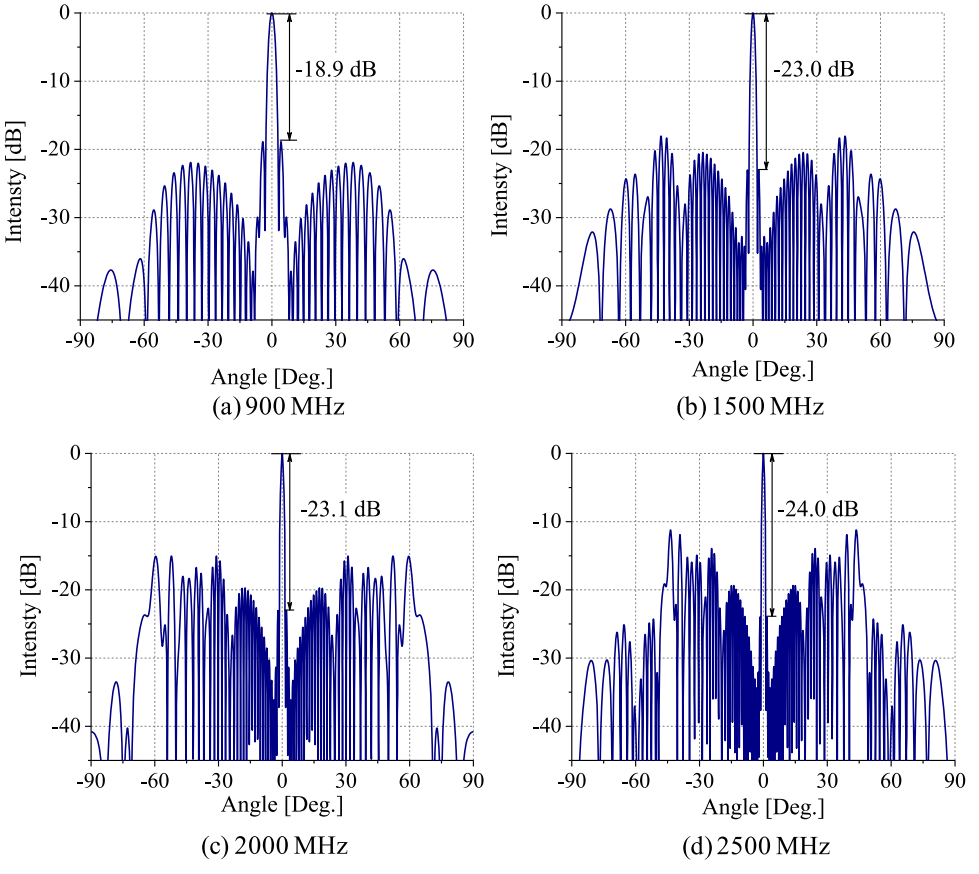

Figure 13. Radiation pattern of the density taper (DTA5).

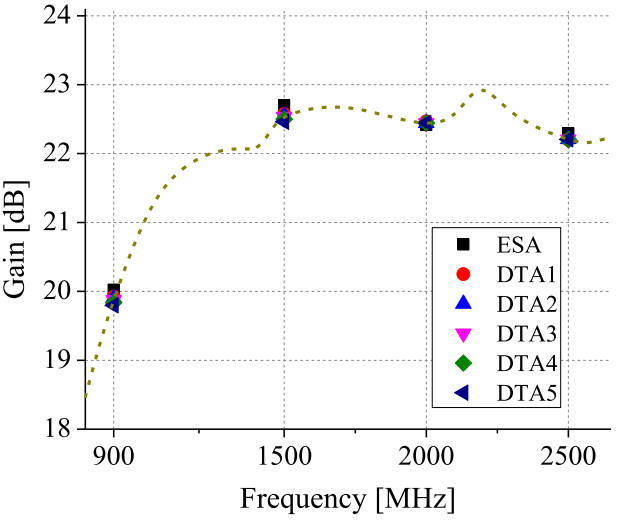

Figure 14. Comparison array gain of ESA and DTAs.

array antenna is used for calculation. At many kinds of density tapering and many frequencies, calculated electric field distributions in a near field region of the array antenna agree with the given density tapering distributions. It is shown that the density tapering is achieved from 900 to 2000 MHz. Moreover, through radiation pattern calculations, effects of grating lobe reductions are ensured from 900 to 2500 MHz.

Disclosure statement

No potential conflict of interest was reported by the author(s).

Funding

This research is funded by Vietnam National Foundation for Science and Technology Development (NAFOSTED) under grant number 102.04-2018.08.

References

[1] Rappaport TS, Sun S, Mayzus K, et al. Millimeter wave mobile communications for 5G cellular: it will Work!. IEEE Access. 2013;1:335–349.
[2] Wang CX, Haider F, Gao X, et al. Cellular architecture and key technologies for 5G wireless communication networks. IEEE Comm Mag. 2014;52:122–130.
[3] Jung YB, Eom SY. A compact multiband and dual-polarized mobile base-station antenna using optimal array structure. Int J Antennas Propagat. 2015;2015:Article ID 178245, 1–11.
[4] Kitchener D, Smith M, Power D, et al. 2001. Multiband terminal and basestation antennas for mobilecommunications. The 11th Int. Conf. on Antennas and Propagat. (ICAP), 2001 April 17–20, Manchester, UK, No. 480, p. 66–71.
[5] Wincza K, Gruszczynski S, Sachse K, et al. Ultrabroadband 8× 8 Butler matrix designed with the use of multisection directional couplers and phase correction networks. Microw Opt Technol Lett. 2012;54(6):1375–1380.
[6] Lee W, Kim J, Yoon YJ. Compact two-layer Rotman lens-fed microstrip antenna array at 24 GHz. IEEE Trans Antennas Propagat. 2011;59(2):460–466.
[7] Yamada Y, Jing CZ, Rahman NHA, et al. Unequally element spacing array antenna with Butler matrix feed for 5G mobile base station. TAFGEN 2018. July 2018;session D251(5) Kuching:72–76.
[8] King D, Packard R, Thomas R. Unequally-spaced, broad-band antenna arrays. IRE Trans Antennas Propagat. 1960;8:380–384.
[9] Bruce JD, Unz H. Broad-band non-uniformly spaced arrays. Proc IRE. 1962;50:228.
[10] Unz H. Linear arrays with arbitrarily distributed elements. IRE Trans Antennas Propagat. 1960;8:222–223.
[11] Unz H. Nonuniformarrays with spacing larger than one wavelength. IRE Trans Antennas Propagat. September 1962;AP-10:647–648.
[12] Harrington RF. Sidelobe reduction by nonuniform element spacing. IRE Trans. March 1961;AP-9:187–192.
[13] Binh NT, Dinh NQ, Yamada Y, et al. 2016. Design of density tapered array for arbitrary density distribution. Int. Conf. on Advanced Technologies for Comm. (ATC), Hanoi, Vietnam, 2016 Oct 12-14, p. 375–379.
[14] Bucci OM, D'Urso M, Isernia T, et al. Deterministic synthesis of uniform amplitude sparse arrays via new density taper techniques. IEEE Trans Antennas Propagat. 2010;58:1949–1958.
[15] Kurup DG, Himdi M, Rydberg A. Synthesis of uniform amplitude unequally spaced antenna arrays using the differential evolution algorithm. IEEE Trans Antennas Propagat. 2003;51:2210–2217.
[16] Lin C, Qing A, Feng Q. Synthesis of unequally spaced antenna arrays by using differential evolution. IEEE Trans Antennas Propagat. 2010;58:2553–2561.
[17] You BQ, Cai LR, Zhou JH, et al. Hybrid approach for the synthesis of unequally spaced array antennas with sidelobes reduction. IEEE Antennas Wirel Propagat Lett. 2015;14:1569–1572.
[18] Collin RE, Zucker FJ. Antenna theory: part 1. New York: McGraw-Hill; 1969.